# A Convex Optimization Approach to Thin Airfoil Design

Daniel C. Berkenstock * and Juan J. Alonso†
*Stanford University, Stanford, CA 94305, USA*

Laurent Lessard‡
*Northeastern University, Boston, MA, 02115, USA*

**Convex optimization techniques can find global optima in polynomial time for problems with convex objective functions and constraints. In this paper, we demonstrate that objective functions involving lift, drag, and moment coefficients may be represented as convex functions when modeled using thin-airfoil theory. Additionally, we describe a rich set of constraints that may be formulated using convex representations. Finally, we apply these methods to the conceptual design of airfoils defined by cubic polynomials. In doing so, we demonstrate the ability to rapidly obtain globally-optimal, up to the limits of parameterization and physical model fidelity, airfoil shapes that maximize supersonic lift-to-drag ratio, given constraints on subsonic lift and moment coefficients, as well as various geometric constraints. Furthermore, we show the ability to expand this method to a bi-level optimization problem, with a single nonconvex variable, identifying a global solution for problems involving the placement of an internal payload. These problems, with up to one thousand constraints, typically run in single-digit seconds on commodity hardware.**

## I. Introduction

THE numerical design of airfoils via optimization has a rich history, beginning with the work of Hicks and Henne [1], Vanderplaats [2], and others in the mid 1970's, when computational resources became powerful enough to repeatedly simulate aerodynamic flows. Such computational capabilities enabled iterative performance improvements, guided by optimization methodologies, via the variation of parameters describing aerodynamic shapes. Since then, methods for Aerodynamic Shape Optimization (ASO) have been expanded dramatically through increasing complexity in shape parameterization, improvements in computational fluid dynamics, multi-fidelity methods, the use of surrogates, and the inexpensive calculation of gradients [3–9]. Today, these methods are routinely applied to the design of complete aircraft configurations [10], often coupled with a variety of additional, non-aerodynamic performance factors [11].

The design of airfoils and other aerodynamic shapes pre-dated the advent of advanced numerical methods by nearly a century [12] and the challenges of marrying the art of aerodynamic shape design with its science have been broadly surveyed over the years [13–15]. Aircraft design, and the design of airfoils by extension, is rarely a one-shot process. Instead, strong coupling between many independent components often leads to an iterative exploration of the design space. Rather than firmly cast from the outset, constraints are often fluid, evolving over the course of the overall design process as new insights demonstrate where small compromises on constraints may lead to significant improvements in performance.

To this end, low-fidelity analysis tools offer the designer an important capability during conceptual design. These tools trade accuracy for speed and, in some cases, provide a guaranteed global optima, at least up to the accuracy of lower-fidelity physical models. Through this approach, it becomes possible to explore the notional impact of a wide variety of geometric or performance constraints on likely performance. Furthermore, the output of these analyses provides a starting point for high-fidelity optimization tools. Using this approach may reduce the number of computationally-expensive, high-fidelity, design steps by providing an initial design that meets all prescribed geometric constraints and is, potentially, already in the neighborhood of a final optimal solution.

In this paper, we explore the benefits and limitations of casting conceptual airfoil design as a convex optimization

*PhD Candidate, Department of Aeronautics and Astronautics.
†Vance D. and Arlene C. Coffman Professor, Department of Aeronautics and Astronautics, AIAA Fellow.
‡Associate Professor, Mechanical and Industrial Engineering.

problem. A convex optimization problem takes the general form

$$\begin{aligned} \underset{x}{\text{minimize}} \quad & f_0(x) \\ \text{subject to} \quad & f_i(x) \leq 0, \ i = 1, \ldots, m, \end{aligned} \tag{1}$$

where $x \in \mathbb{R}^n$ is a vector of design variables and the $f_i : \mathbb{R}^n \to \mathbb{R}$ are convex objective and constraint functions. A function $f : \mathbb{R}^n \to \mathbb{R}$ is convex if the domain of $f$ ($\text{dom} f$) is a convex set and if for all $x, y \in \text{dom} f$, with $0 \leq \theta \leq 1$,

$$f(\theta x + (1-\theta)y) \leq \theta f(x) + (1-\theta) f(y). \tag{2}$$

Geometrically, this indicates that the function lies below the line segment connecting any two points of its graph. For a complete overview of convex optimization and convex functions we refer the reader to the book by Boyd and Vandenberghe [16]. A list of common convex functions and their domains is included in Table 1.

| **Function** | **Definition** | **Domain** | **Curvature** |
|---|---|---|---|
| Summation | $\sum_{ij} X_{ij}$ | $X \in \mathbb{R}^{m \times n}$ | convex |
| Max | $\max_{ij}\{X_{ij}\}$ | $X \in \mathbb{R}^{m \times n}$ | convex |
| Min | $\min_{ij}\{X_{ij}\}$ | $X \in \mathbb{R}^{m \times n}$ | concave |
| 2-norm | $\sqrt{\sum_i x_i^2}$ | $x \in \mathbb{R}^n$ | convex |
| Positive semidefinite quadratic form | $x^T P x$ | $x \in \mathbb{R}^n$, $P \succeq 0$ | convex |
| Quadratic over linear | $x^T x / y$ | $x \in \mathbb{R}^n$, $y > 0$ | convex |
| Inverse positive | $1/x$ | $x > 0$ | convex |

**Table 1 Representative convex functions**

Convex optimization has been used in a variety of fields spanning finance [17], control theory [18], circuit layout [19], and structural design [20]. In aircraft design, it has been primarily employed in the design of complete aircraft by Hoburg et al. [21] and Burton et al. [22].

There are several reasons for the strong interest in using convex optimization methods in conceptual airfoil design. First, within the limitations of the simplified physics which may be modeled by convex functions, convex optimization provides certifiably global optima. Second, this approach does not require an initial design point and is not subject to convergence difficulties if the initial guess is not close to either satisfying optimality and/or feasibility criteria. Finally, a variety of readily-available convex optimization solvers are capable of solving problems with thousands of design variables and/or constraints in seconds on a standard laptop computer, providing the designer with the ability to run many iterations of a problem as they explore the impact of problem formulation alternatives, different shape parameterization and large ranges of constraint values.

The benefits of this approach come at a price; so far, the limitation to convex objective and constraint functions precludes use of numerical solutions of the partial differential equations that describe fluid flows with higher fidelity. With those limitations in mind, a detailed examination of linearized, classical descriptions of aerodynamic performance indicators show that many may be cast as convex functions. Despite the simplicity in the physical modeling of such methods, they serve as a starting point to consider more advanced methods that can leverage the benefits of convexity in higher-fidelity formulations. In addition, these simplified approaches can be used in combination with higher-fidelity ASO techniques to accelerate convergence to an optimum design.

Thin-airfoil theory, in particular, finds itself well suited to a convex optimization approach. In both the subsonic and supersonic flight regimes, thin-airfoil theory provides linear approximations to sectional lift and moment, for shapes that are defined as a linear combination of design variables with basis functions. Even in recent years, these classical results have been expanded to improve accuracy over a broader range of thicknesses [23] and to identify closed form solutions for generic camber definitions [24]. Moreover, due to the linear behavior of lift and the quadratic nature of induced drag in three-dimensional inviscid areodynamic theories, convex optimization is also likely to be usable in those contexts.

In this paper, we make several contributions. First, we derive closed-form solutions for lift, drag, and moment coefficients using thin-airfoil theory, across several flow regimes, for the case of airfoils whose shape is defined by two

cubic polynomials. We also show that important performance indicators, under these assumptions, are convex functions. Next, we demonstrate that a variety of useful constraints on airfoil geometry may be stated as convex constraints. Finally, we present several case studies that illustrate our proposed approach. Each case study draws from a flexible menu of performance indicators and geometric constraints, and is solved to global optimality using using readily available commercial software.

Our hope with this paper is to begin investigations leading to more widespread use of convex optimization techniques in aerodynamic shape optimization problems.

## II. Application of Thin-Airfoil Theory to Polynomial Airfoils

In this work, we will consider *polynomial airfoils*, which are airfoils defined by separate polynomials representing the upper and lower surfaces:

$$y_u(x) = \sum_{k=0}^{n} a_k x^k \qquad \text{and} \qquad y_l(x) = \sum_{k=0}^{n} b_k x^k. \tag{3}$$

Our approach is general and can be used with polynomials of arbitrary degree. However, for simplicity and ease of exposition, we will restrict ourselves to cubic polynomials for the remainder of the paper, so

$$y_u(x) = a_3x^3 + a_2x^2 + a_1x + a_0 \qquad \text{and} \qquad y_l(x) = b_3x^3 + b_2x^2 + b_1x + b_0, \tag{4}$$

where, in order to ensure a closed shape, both surfaces must meet at the leading and trailing edges of the airfoil, separated by the aerodynamic chord, which without loss of generality we assume to have length equal to 1:

$$y_u(0) = y_l(0) = 0 \qquad \text{and} \qquad y_u(1) = y_l(1) = 0. \tag{5}$$

Each surface has only two independent parameters, and (3) reduces to

$$y_u(x) = -(a_1 + a_2)x^3 + a_2x^2 + a_1x, \qquad \text{and} \qquad y_l(x) = -(b_1 + b_2)x^3 + b_2x^2 + b_1x. \tag{6}$$

Employing (6), Figure 1 shows a set of derived airfoil shapes, sampled across $(a_1, a_2, b_1, b_2) \subset \mathbb{R}^4$, showing that a broad range of airfoil thickness and camber distributions can be represented by this parameterization. Moreover, using the polynomial representation, other typical airfoil properties such at the the leading edge radius, the trailing edge included angle, and the trailing edge bisector slope can be captured by combinations of the parameters of the polynomials.

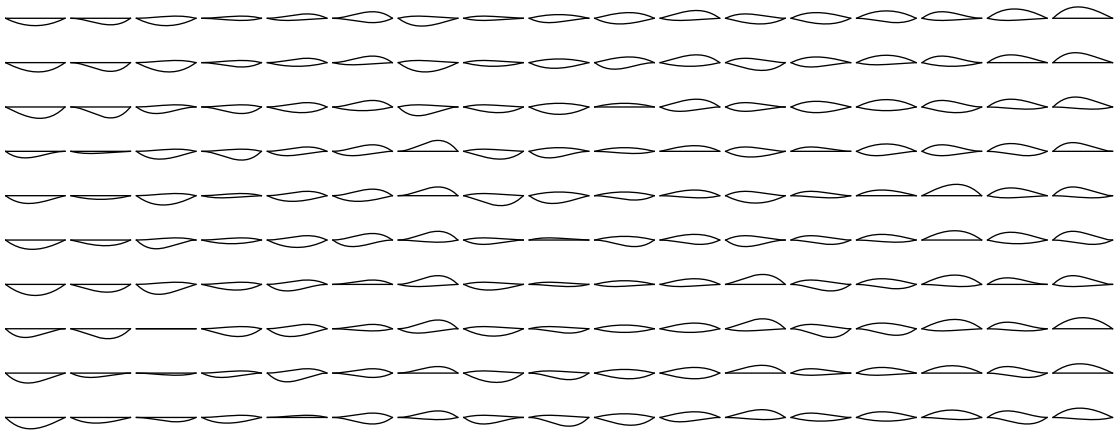

**Fig. 1 Sample airfoils from the $\mathbb{R}^4$ design space**

We will now analyze the aerodynamic properties of cubic airfoils in subsonic and supersonic flows. In each circumstance we will employ thin-airfoil theory, under which we assume the thickness and camber of the airfoil is small compared to the chord. In addition, we also implicitly assume that the leading-edge radius of the airfoil is small.

### A. Thin Airfoil Aerodynamics: Subsonic Cubic Airfoils

Thin-airfoil theory provides closed form analytic solutions for the lift and moment coefficients of a reasonably thin airfoil in a subsonic, invsicid, irrotational, incompressible flow. As presented in [25], the sectional lift and moment coefficients are dependent solely upon the shape of the camber line:

$$z(x) = \frac{y_u(x) + y_l(x)}{2} = \frac{-(a_1 + a_2 + b_1 + b_2)x^3 + (a_2 + b_2)x^2 + (a_1 + b_1)x}{2}, \tag{7}$$

and its slope

$$\frac{\mathrm{d}z}{\mathrm{d}x} = \frac{-3(a_1 + a_2 + b_1 + b_2)x^2 + 2(a_2 + b_2)x + (a_1 + b_1)}{2}. \tag{8}$$

For ease of integration, we employ the conventional cosine transformation $x = \frac{1}{2}(1 - \cos\theta)$, so that, once simplified,

$$\frac{\mathrm{d}z}{\mathrm{d}x} = (a_1 + a_2 + b_1 + b_2)\left(3\sin^4\left(\tfrac{\theta}{2}\right) - 1\right) - (a_2 + b_2)\cos\theta. \tag{9}$$

The sectional lift coefficient is $c_l = 2\pi(\alpha - \alpha_{l0})$, where the angle of zero lift is given by

$$\alpha_{l0} = \frac{1}{\pi}\int_0^\pi \frac{\mathrm{d}z}{\mathrm{d}x}(1 - \cos\theta)\,\mathrm{d}\theta. \tag{10}$$

The moment coefficient about the aerodynamic center is

$$c_{\mathrm{m_{ac}}} = -\frac{1}{2}\int_0^\pi \frac{\mathrm{d}z}{\mathrm{d}x}(\cos\theta - \cos 2\theta)\,\mathrm{d}\theta. \tag{11}$$

Evaluating the above integrals, we obtain

$$\alpha_{l0} = -\frac{1}{16}(7a_1 + 3a_2 + 7b_1 + 3b_2), \tag{12}$$

$$c_{\mathrm{m_{ac}}} = -\frac{\pi}{64}(15a_1 + 7a_2 + 15b_1 + 7b_2), \tag{13}$$

$$c_l = 2\pi\left(\alpha + \frac{1}{16}(7a_1 + 3a_2 + 7b_1 + 3b_2)\right). \tag{14}$$

For this subsonic case, and under thin airfoil assumptions, $c_l$, $c_{\mathrm{mac}}$, and $\alpha_{l0}$ are affine, and therefore convex, functions of the polynomial coefficients $a_i$ and $b_i$ and the angle of attack $\alpha$. The same holds true when the cubic polynomials are replaced by higher-order polynomials. In fact, this holds whenever $y_u(x)$ and $y_l(x)$ are linear functions of the $a_i$ and $b_i$, respectively. So we can replace the functions $\{1, x, x^2, x^3\}$ by any set of integrable functions of $x$. We also note that, for subsonic thin-airfoil theory, the predicted drag (and drag coefficient) is zero. Accounting for viscous-related drag is a challenge that we intend to tackle in the future.

### B. Thin Airfoil Aerodynamics: Supersonic Cubic Airfoils

As presented in [26], under suitable assumptions including small thickness, camber, and angle of attack and sharp leading edges, the lift and drag coefficients of an airfoil in a supersonic flow may be approximated as

$$c_l = \frac{4\alpha}{\sqrt{M^2 - 1}} \qquad \text{and} \qquad c_d = \frac{4}{\sqrt{M^2 - 1}}\left(\alpha^2 + K_2 + K_3\right). \tag{15}$$

Here we will again assume a chord length of 1. The $K_2$ term accounts for wave drag created by the camber line,

$$K_2 = \int_0^1 \left[\frac{\mathrm{d}}{\mathrm{d}x}\left(\frac{y_u(x) + y_l(x)}{2}\right)\right]^2 \mathrm{d}x, \tag{16}$$

and the $K_3$ term accounts for wave drag generated by the airfoil thickness,

$$K_3 = \int_0^1 \left[\frac{\mathrm{d}}{\mathrm{d}x}\left(\frac{y_u(x) - y_l(x)}{2}\right)\right]^2 \mathrm{d}x. \tag{17}$$

Evaluating these terms for the cubic case, we find that

$$K_2 = \frac{1}{60}\left(12a_1^2 + 2a_2^2 + 9a_2b_1 + 12b_1^2 + 4a_2b_2 + 9b_1b_2 + 2b_2^2 + 3a_1(3a_2 + 8b_1 + 3b_2)\right), \tag{18}$$

$$K_3 = \frac{1}{60}\left(12a_1^2 + 2a_2^2 - 9a_2b_1 + 12b_1^2 + 3a_1(3a_2 - 8b_1 - 3b_2) - 4a_2b_2 + 9b_1b_2 + 2b_2^2\right). \tag{19}$$

Substituting (18)–(19) into (15), we see that the drag coefficient may be represented as a quadratic form in the polynomial coefficients and the angle of attack. Specifically, $c_d = \frac{4}{\sqrt{M^2-1}} v^T Q v$, where

$$Q = \begin{bmatrix} 1 & 0 & 0 & 0 & 0 \\ 0 & \frac{2}{5} & \frac{3}{20} & 0 & 0 \\ 0 & \frac{3}{20} & \frac{1}{15} & 0 & 0 \\ 0 & 0 & 0 & \frac{2}{5} & \frac{3}{20} \\ 0 & 0 & 0 & \frac{3}{20} & \frac{1}{15} \end{bmatrix} \qquad \text{and} \qquad v = \begin{bmatrix} \alpha \\ a_1 \\ a_2 \\ b_1 \\ b_2 \end{bmatrix}. \tag{20}$$

It is straightforward to check that all eigenvalues of $Q$ are positive, and so $Q$ is positive definite, and $c_d$ is a convex function of $v$.

Given that the lift coefficient is represented by a linear function in supersonic thin-airfoil theory, the drag-to-lift ratio is the ratio of a quadratic to a linear function,

$$\frac{D}{L} = \frac{v^T Q v}{\alpha}. \tag{21}$$

Per the above analysis, this is, in fact, the ratio of a *positive definite* quadratic over a linear function. Therefore, imposing an upper bound on $D/L$ (or equivalently, a lower bound on $L/D$) over the set $\{\alpha > 0\}$ is convex-representable.*

Finally, the moment coefficient about the aerodynamic center for the supersonic thin airfoil case is

$$c_{m_{ac}} = \frac{4K_1}{\sqrt{M^2-1}}, \qquad \text{where} \qquad K_1 = \int_0^1 \left[\frac{\mathrm{d}}{\mathrm{d}x}\left(\frac{y_u(x) + y_l(x)}{2}\right)\right] x \,\mathrm{d}x. \tag{22}$$

For the cubic airfoil case, this evaluates to

$$c_{m_{ac}} = -\frac{1}{6\sqrt{M^2-1}}\left(3a_1 + a_2 + 3b_1 + b_2\right), \tag{23}$$

which is a linear, and therefore convex, function of the parameters defining the airfoil.

Careful examination of (15)–(17) reveals that $c_d$ will be a convex quadratic function of the airfoil polynomial coefficients $a_i$ and $b_i$ and the angle of attack $\alpha$ even for higher-order polynomials or when using a non-polynomial basis as was true in the subsonic case. The same holds for upper-bounding $D/L$ (or lower-bounding $L/D$), and for $c_{m_{ac}}$.

## III. Geometric Constraints

A number of useful geometric constraints may be modeled as constraints that are convex in the parameters of the airfoil. In some cases, these are an individual constraint, while in others they are multiple constraints, sampled uniformly over the chord of the airfoil. A variety of these constraints are described below.

### A. Single Constraints

The constraints described in this section describe integrated quantities over the complete airfoil section.

#### *1. Minimum Area*

The enclosed area of an airfoil represents the amount of payload that could be contained within, especially in the case that payload is a liquid, such as fuel. This integrated area can also be used as a surrogate for the structural depth of the section. The area is calculated as the integral of the thickness between the upper and lower surfaces over the airfoil,

*It may be written as the *perspective* of the squared Euclidean norm [16, §3.2.6].

$$A = \int_0^1 (y_u(x) - y_l(x))\,\mathrm{d}x = \int_0^1 \left(-(a_1 + a_2 - b_1 - b_2)x^3 + (a_2 - b_2)x^2 + (a_1 - b_1)x\right)\,\mathrm{d}x. \tag{24}$$

This leads to the affine constraint $\frac{1}{12}(3a_1 + a_2 - 3b_1 - b_2) \geq A_{\min}$.

*2. Arc Length*

The arc length of a cubic polynomial does not have a readily available closed form solution, as

$$l = \int_0^1 \sqrt{1 + \left(\frac{\mathrm{d}y}{\mathrm{d}x}\right)^2}\,\mathrm{d}x \tag{25}$$

results in an elliptic integral. However, the arc length may be approximated to arbitrary precision as a summation of norms, resulting in the convex constraints,

$$\sum_i \left\| \begin{bmatrix} y_u(x_{i+1}) - y_u(x_i) \\ x_{i+1} - x_i \end{bmatrix} \right\| \leq l_{u_{\max}} \qquad \text{and} \qquad \sum_i \left\| \begin{bmatrix} y_l(x_{i+1}) - y_l(x_i) \\ x_{i+1} - x_i \end{bmatrix} \right\| \leq l_{l_{\max}}. \tag{26}$$

**B. Sampled Constraints**

The constraints described in this section reflect properties across a range of $x$ values. For example, if we are interested in some property $g(x, v)$ that depends on the position $x$ along the chord and the airfoil parameters $v$ (e.g., the polynomial coefficients $a_i$ and $b_i$), constraints that bound the maximum or minimum over some subset $x \in S$ of possible $x$ values would take the form

$$\max_{x \in S} g(x, v) \leq g_{\max} \qquad \text{or} \qquad \min_{x \in S} g(x, v) \geq g_{\min}. \tag{27}$$

These constraints are convex in $v$ provided $g$ is a convex function of $v$ (for the $g_{\max}$ constraint) or $g$ is a concave function of $v$ (for the $g_{\min}$ constraint). Indeed, (27) can be rewritten as

$$g(x, v) \leq g_{\max} \quad \text{for all } x \in S, \qquad \text{or} \qquad g(x, v) \geq g_{\min} \quad \text{for all } x \in S. \tag{28}$$

When $g$ is an affine function of $v$, both constraints are convex. However, these constraints can be difficult to incorporate into a numerical solver because when $S$ contains infinitely many points, such as within an interval $S = [x_1, x_2]$, the constraints (28) correspond to infinitely many constraints (one for each $x \in S$). This limitation can be overcome by *sampling*. In other words, we pick a finite set of representative points $\{x_1, x_2, \ldots, x_m\} \subset S$ and instead impose the constraints

$$g(x_k, v) \leq g_{\max} \quad \text{for } k = 1, \ldots, m, \qquad \text{or} \qquad g(x_k, v) \geq g_{\min} \quad \text{for } k = 1, \ldots, m. \tag{29}$$

Below we describe some examples of constraints that can be modeled in this fashion and their associated $g$ functions.

*1. Thickness*

Often it is desirable to place minimum or maximum limits on the thickness, $\tau = y_u - y_l$, of an airfoil. These constraints may be specified over the entire airfoil, or a region, $x \in [x_1, x_2]$, and the corresponding $g$ function is

$$g(x) = -(a_1 + a_2 - b_1 - b_2)x^3 + (a_2 - b_2)x^2 + (a_1 - b_1)x. \tag{30}$$

This function is affine in the airfoil parameters, so we can impose either upper or lower bound constraints. In order to prevent unwanted intersections between the upper and lower surfaces, it is generally advisable to include the constraint $g(x) \geq 0$ for $x \in [0, 1]$.

*2. Gradient and Curvature Constraints*

It may be desirable to place limitations on the derivatives of the shape, for instance in order to prevent large pressure gradients that may lead to flow separation. This may be done for curvature (second derivative, more relevant in subsonic flow) using the $g$ function

$$g(x) = -6(a_1 + a_2)x + 2a_2, \tag{31}$$

or for the gradient (first derivative, more relevant in supersonic flow) using the $g$ function

$$g(x) = -3(a_1 + a_2)x^2 + 2a_2x + a_1. \tag{32}$$

These functions are affine in the airfoil parameters, so we can impose upper or lower bound constraints on either one.

*3. Internal Payloads*

Beyond the constraints discussed above, a designer may want to ensure that various shapes are able to fit into the internal cavity of the airfoil. For instance, a circle of radius, $r$, centered at $[x_c, y_c]$, can be prescribed by including the following sampled constraints, which correspond to the upper and lower surfaces, respectively:

$$g(\theta) = \begin{cases} -(a_1 + a_2)(x_c + r\cos\theta)^3 + a_2(x_c + r\cos\theta)^2 + a_1(x_c + r\cos\theta) - y_c - r\sin\theta) \geq 0 & \text{for all } \theta \in [0, \pi] \\ -(b_1 + b_2)(x_c + r\cos\theta)^3 + b_2(x_c + r\cos\theta)^2 + b_1(x_c + r\cos\theta) - y_c - r\sin\theta) \leq 0 & \text{for all } \theta \in [\pi, 2\pi]. \end{cases} \tag{33}$$

An internal square constraint may be defined as a minimum thickness constraint over a window centered at $x_c$ and $y_c$. For constant $x_c$, $y_c$, and $r$ these each describe affine constraints.

## IV. Application to Airfoil Design

In the previous sections, we have provided an overview of several indicators of performance and a number of constraints that may be modeled as convex functions of the parameters of a given thin, polynomial airfoil. To summarize the previous sections, Table 2 highlights a subset of objective functions and constraints that can be easily included in convex optimization problems for airfoil design based on thin-airfoil theory. The power of this approach lies in the ability to pick arbitrarily from this menu since any convex combination of convex functions is also convex.

| **Aerodynamic Performance** | **Geometric Constraints** |
|---|---|
| Subsonic lift coefficient | Minimum/Maximum thickness |
| Subsonic moment coefficient | Minimum/Maximum area |
| Supersonic drag coefficient | Minimum/Maximum gradient |
| Supersonic lift to drag ratio | Minimum/Maximum curvature |
| Supersonic moment coefficient | Internal payload constraints |
| | Non-Intersection constraint |
| | Maximum arc length constraint |

**Table 2 Design of thin, polynomial airfoils: convex objectives and constraints**

In the remainder of this paper, we demonstrate applications of this approach using several examples of increasing complexity. First, we consider minimization of drag of a zero lift airfoil in a supersonic flow, a problem with a convex quadratic objective function and linear constraints. Then, we demonstrate the ability to maximize the lift to drag ratio for a thin airfoil in supersonic flow, a problem with a convex, quadratic over linear objective function and linear constraints. Next, we combine both flow regimes, maximizing lift to drag ratio for a supersonic airfoil subject to a minimum subsonic lift coefficient constraint in addition to geometric constraints. Finally, we demonstrate the extension of this approach to a bi-level optimization problem, including a single nonconvex variable.

### A. Solving Convex Optimization Problems

Packages such as CVXPY [27, 28] and YALMIP [29] are modeling languages for convex optimization that efficiently and automatically transform a problem into a standard form, call an external solver, and post-process the results. As an example, consider the problem of maximizing the area under a cubic airfoil $y_u(x) = -(a_1 + a_2)x^3 + a_2x^2 + a_1x$ which has a flat lower surface $y_l(x) = 0$, and obeys the thickness constraint $y_u(x) \leq 0.2$ whenever $0 \leq x \leq 0.4$. This problem

may be expressed as the optimization problem

$$\begin{aligned}
\underset{\{a_1,a_2\}}{\text{maximize}} \quad & \frac{1}{12}(3a_1 + a_2) && \text{(function describing the area)} \\
\text{subject to} \quad & \max_{x\in[0,0.4]} \left(-(a_1 + a_2)x^3 + a_2x^2 + a_1x\right) \leq 0.2 && \text{(thickness constraint)} \\
& \min_{x\in[0,1]} \left(-(a_1 + a_2)x^3 + a_2x^2 + a_1x\right) \geq 0 && \text{(non-intersection constraint)}
\end{aligned} \tag{34}$$

The solution, employing uniformly sampled maximum thickness and non-intersection constraints, is shown in Figure 2. The maximum area is $A_{\max} = 0.174$, which is achieved when $a_1 = -0.002$ and $a_2 = 2.091$.

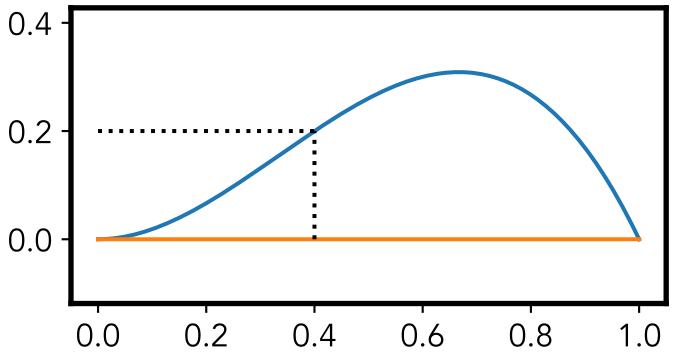


**Fig. 2 Maximum area airfoil subject to a partial thickness constraint**

### B. Minimum Drag Supersonic Airfoil

Moving on to a more realistic example, consider the well-known case of minimizing the drag of a supersonic, non-lifting airfoil. Formally, we seek to minimize drag subject to a non-intersection constraint and a minimum area constraint, which may be formulated, with vector of design variables $v^T = [\alpha, a_1, a_2, b_1, b_2]$, as

$$\begin{aligned}
\underset{v}{\text{minimize}} \quad & \frac{4v^TQv}{\sqrt{M^2 - 1}} \\
\text{subject to} \quad & \min_{x\in[0,1]} \left(-(a_1 + a_2 - b_1 - b_2)x^3 + (a_2 - b_2)x^2 + (a_1 - b_1)x\right) \geq 0 \\
& \frac{1}{12}(3a_1 + a_2 - 3b_1 - b_2) \geq A_{\min}.
\end{aligned} \tag{35}$$

In this example, we specify $M = 2$ and $A_{\min} = 0.075$, with a constraint sampling interval $\Delta x = 0.01$. The resulting airfoil is shown in Figure 3. The globally optimal parameters for the airfoil shape are $a_1 = 0.225$, $a_2 = -0.225$, $b_1 = -0.225$, and $b_2 = 0.225$, with a resulting drag coefficient, $c_d = 0.039$.[†]

In fact, for this simple example, the results may be verified analytically. Here, the area constraint will be an active, and therefore equality constraint, and the specification of a minimum area will render the non-intersection constraint unnecessary. Given these modifications, we can restate the problem as,

$$\begin{aligned}
\underset{v}{\text{minimize}} \quad & \frac{4v^TQv}{\sqrt{M^2 - 1}} \\
\text{subject to} \quad & 3a_1 + a_2 - 3b_1 - b_2 = 12A_{\min}.
\end{aligned} \tag{36}$$

As this problem now requires the minimization of a quadratic function, subject to a linear equality constraint, we may consider solving the unconstrained minimization of the augmented Lagrangian,

$$\underset{v,\lambda}{\text{minimize}} \quad \frac{4v^TQv}{\sqrt{M^2 - 1}} - \lambda(12A_{\min} - 3a_1 + a_2 - 3b_1 - b_2). \tag{37}$$

[†]This recovers a bi-convex profile which is the closest representable shape, using cubic polynomials, to the well-known theoretical minimum profile drag shape, in a supersonic flow, of a symmetrical wedge [26, §12.6.3].

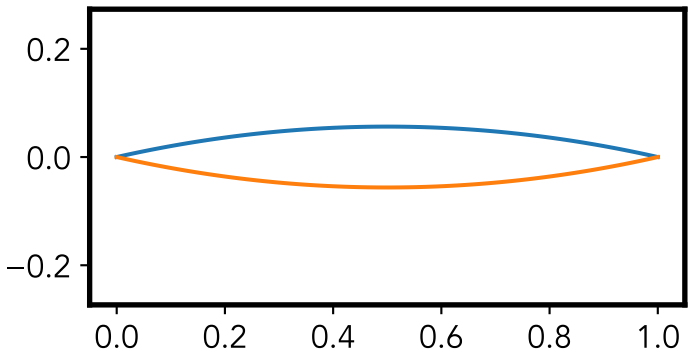


**Fig. 3 Minimum supersonic drag cubic airfoil subject to thickness and area constraints**

This problem may be solved in closed form, by setting the gradient to zero, and solving a linear system, where $c^T = [0, 3, 1, -3, -1]$,

$$\begin{bmatrix} Q & c \\ c^T & 0 \end{bmatrix} \begin{bmatrix} v_{\text{opt}} \\ \lambda \end{bmatrix} = \begin{bmatrix} 0 \\ 12A_{\min} \end{bmatrix}, \tag{38}$$

which recovers the previous answer, $v_{\text{opt}}^T = [0.0, .0225, -0.225, -0.225, 0.225]$, with $\lambda = -3/(40\sqrt{M^2 - 1})$.

### C. Maximum Lift-to-Drag Ratio Supersonic Airfoil with Internal Payload

As a second example, we consider the case of maximizing the lift-to-drag ratio of a lifting supersonic airfoil, now with an internal payload and thickness constraint, in addition to the previous non-intersection constraint. This problem is formulated as

$$\begin{aligned}
\underset{v}{\text{minimize}} \quad & \frac{v^T Q v}{\alpha} \\
\text{subject to} \quad & \min_{x\in[0,1]} \left(-(a_1 + a_2 - b_1 - b_2)x^3 + (a_2 - b_2)x^2 + (a_1 - b_1)x\right) \geq 0 \\
& \max_{x\in[0,1]} \left(-(a_1 + a_2 - b_1 - b_2)x^3 + (a_2 - b_2)x^2 + (a_1 - b_1)x\right) \leq \tau_{\max} \\
& \min_{\theta\in[0,\pi]} \left(-(a_1 + a_2)(x_c + r\cos\theta)^3 + a_2(x_c + r\cos\theta)^2 + a_1(x_c + r\cos\theta) - y_c - r\sin\theta\right) \geq 0 \\
& \max_{\theta\in[\pi,2\pi]} \left(-(b_1 + b_2)(x_c + r\cos\theta)^3 + b_2(x_c + r\cos\theta)^2 + b_1(x_c + r\cos\theta) - y_c - r\sin\theta\right) \leq 0 \\
& \frac{1}{12}(3a_1 + a_2 - 3b_1 - b_2) \geq A_{\min} \\
& \alpha \geq 0.
\end{aligned} \tag{39}$$

In this example, we specify $M = 2$, $\tau_{\max} = 0.175$, $r = 0.075$, $x_c = 0.25$, and $y_c = 0.0$, with a constraint sampling interval $\Delta x = 0.01$. The resulting airfoil is shown in Figure 4. In this case, the optimal parameters for the airfoil shape are $\alpha = 11.17°$, $a_1 = 0.524$, $a_2 = -1.01$, $b_1 = -0.524$, and $b_2 = 1.01$. The maximum lift to drag ratio is $\text{L/D}_{\max} = 5.89$.

### D. Maximum Lift-to-Drag Ratio Supersonic Airfoil with Subsonic Lift and Moment Constraints

In the next example, we expand the constraint set to include a minimum subsonic lift coefficient and maximum subsonic moment about the aerodynamic center. Under the cubic polynomial parameterization, this is essentially an academic result as an optimal subsonic result will require a rounded leading edge. Future parameterizations, including

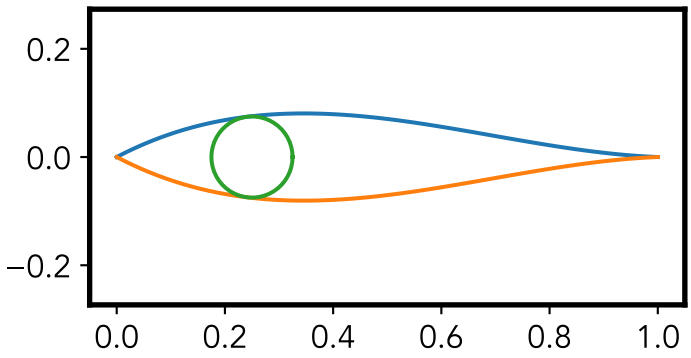


**Fig. 4 Maximum supersonic lift-to-drag ratio cubic airfoil including internal payload constraints**

cubic splines, will address this issue. The problem now may be stated as

$$
\begin{aligned}
\underset{v}{\text{minimize}} \quad & \frac{v^T Q v}{\alpha} \\
\text{subject to} \quad & \min_{x\in[0,1]} \left(-(a_1+a_2-b_1-b_2)x^3+(a_2-b_2)x^2+(a_1-b_1)x\right) \geq 0 \\
& \max_{x\in[0,1]} \left(-(a_1+a_2-b_1-b_2)x^3+(a_2-b_2)x^2+(a_1-b_1)x\right) \leq \tau_{\max} \\
& \min_{\theta\in[0,\pi]} \left(-(a_1+a_2)(x_c+r\cos\theta)^3+a_2(x_c+r\cos\theta)^2+a_1(x_c+r\cos\theta)-y_c-r\sin\theta\right) \geq 0 \\
& \max_{\theta\in[\pi,2\pi]} \left(-(b_1+b_2)(x_c+r\cos\theta)^3+b_2(x_c+r\cos\theta)^2+b_1(x_c+r\cos\theta)-y_c-r\sin\theta\right) \leq 0 \\
& \frac{1}{12}(3a_1+a_2-3b_1-b_2) \geq A_{\min} \\
& 2\pi\left(\alpha+\frac{1}{16}(7a_1+3a_2+7b_1+3b_2)\right) \geq c_{l_{\min}} \\
& -\frac{\pi}{64}(15a_1+7a_2+15b_1+7b_2) \leq c_{m_{\max}} \\
& \alpha \geq 0.
\end{aligned}
\tag{40}
$$

In this example, we specify $M = 2$, $\tau_{\max} = 0.175$, $r = 0.075$, $x_c = 0.25$, $y_c = 0.0$, $c_{l_{\min}} = 2.5$, and $c_{m_{\max}} = -0.075$, with a constraint sampling interval $\Delta x = 0.01$. The solution to this problem is shown in Figure 5. In this case, the optimal parameters for the airfoil shape are $\alpha = 18.33°$, $a_1 = 0.45$, $a_2 = -0.63$, $b_1 = -0.60$, and $b_2 = 1.39$. The maximum supersonic lift-to-drag ratio is $\mathrm{L/D}_{\max} = 5.01$.

### E. Maximum Lift-to-Drag Ratio Supersonic Airfoil with Variable Internal Payload

This approach offers benefits for other problems which are also not strictly convex, or at least readily identifiable as convex. For instance, a natural extension of the previous problem is to determine the optimal placement of an internal

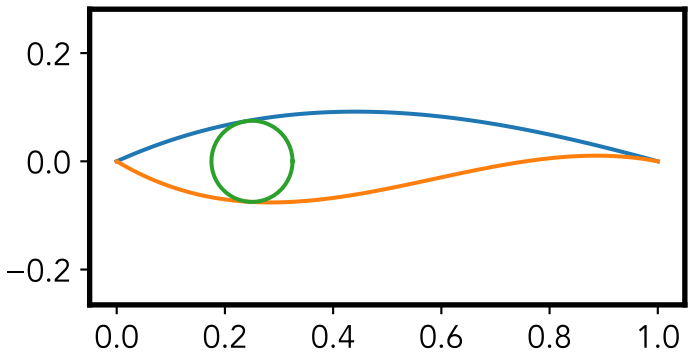


**Fig. 5 Maximum supersonic lift-to-drag ratio cubic airfoil subject to subsonic constraints**

payload, in addition to the maximum lift-to-drag ratio under that placement, or

$$
\begin{aligned}
\underset{\{v,x_c,y_c\}}{\text{minimize}} \quad & \frac{v^T Q v}{\alpha} \\
\text{subject to} \quad & \min_{x\in[0,1]} \left(-(a_1+a_2-b_1-b_2)x^3+(a_2-b_2)x^2+(a_1-b_1)x\right) \geq 0 \\
& \max_{x\in[0,1]} \left(-(a_1+a_2-b_1-b_2)x^3+(a_2-b_2)x^2+(a_1-b_1)x\right) \leq \tau_{\max} \\
& \min_{\theta\in[0,\pi]} \left(-(a_1+a_2)(x_c+r\cos\theta)^3+a_2(x_c+r\cos\theta)^2+a_1(x_c+r\cos\theta)-y_c-r\sin\theta\right) \geq 0 \\
& \max_{\theta\in[\pi,2\pi]} \left(-(b_1+b_2)(x_c+r\cos\theta)^3+b_2(x_c+r\cos\theta)^2+b_1(x_c+r\cos\theta)-y_c-r\sin\theta\right) \leq 0 \\
& \frac{1}{12}(3a_1+a_2-3b_1-b_2) \geq A_{\min} \\
& 2\pi\left(\alpha+\frac{1}{16}(7a_1+3a_2+7b_1+3b_2)\right) \geq c_{l_{\min}} \\
& -\frac{\pi}{64}(15a_1+7a_2+15b_1+7b_2) \leq c_{m_{\max}} \\
& \alpha \geq 0.
\end{aligned}
\tag{41}
$$

This problem remains convex in $y_c$, since $y_c$ only appears as a linear term in the set of constraints. However, multiple nonlinear terms are introduced as products of $a_i x_c^k$, which are not obviously convex. Hence, it is possible to approach this as a bi-level problem, with a convex inner layer, and a single design variable in the outer loop, $x_c$. This can be solved by coupling the inner, convex, solution with a golden search approach in the outer layer.

The results of this approach are shown below, with specifications that $r = 0.025$, $c_{l_{\min}} = 1.5$, and $c_{m_{\max}} = -0.15$. First, Figure 7 shows the swept curve of maximum achievable L/D as a function of $x_c$, along with the point of overall maximum lift to drag and the overall convergence rate. Then, Figure 8 shows the resulting optimal airfoil. The optimal $\text{L/D}_{\max} = 10.56$, which occurs at approximately $x_c = 0.520$, $y_c = 0.029$, and $\alpha = 8.98°$. Although not readily apparent, the optimal lift to drag does appear to be concave in $x_c$, an exercise we will leave to a future paper to prove.

## V. Performance Benchmarking

In this section, we briefly describe typical solution times for the problems outlined above. In Figure 9, we show the solution times and residual for a variety of solutions of a maximum supersonic lift-to-drag airfoil featuring a circular, internal payload. In order to assess the effect on the final solution of linear constraint sampling, we ran a given configuration multiple times while using an increasingly fine sampling value for the angle, $\theta$ used to resolve the circular constraint. As can be seen below, problems with more than one thousand linear constraints, and six design variables, ran in single digit seconds on a 2.9 Ghz, Intel Quadcore Macbook. Similarly, the solution converged quickly, using a relatively small number of linear constraint samples.

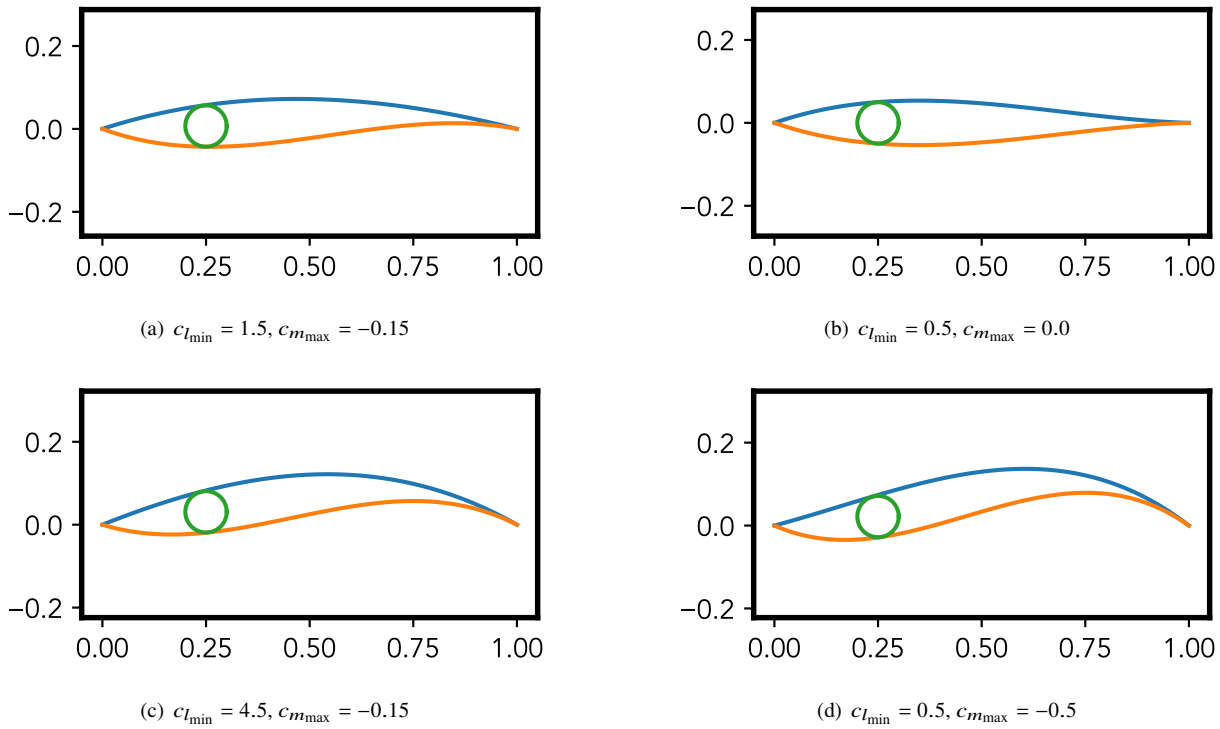


(a) $c_{l_{\min}} = 1.5$, $c_{m_{\max}} = -0.15$

(b) $c_{l_{\min}} = 0.5$, $c_{m_{\max}} = 0.0$

(c) $c_{l_{\min}} = 4.5$, $c_{m_{\max}} = -0.15$

(d) $c_{l_{\min}} = 0.5$, $c_{m_{\max}} = -0.5$

**Fig. 6 Optimal airfoil design for various subsonic moment and lift constraints** ($M = 2$, $r = 0.05$, $x_c = 0.25$)

## VI. Conclusion

In this paper, we have presented an approach to conceptual airfoil design, in circumstances where the assumptions of thin-airfoil theory hold, that provides global optima in polynomial time using convex optimization techniques. These techniques provide the designer with a ready menu of options for objective function and constraints that allow for the application of a variety of aerodynamic and geometric constraints. The resulting problems may be solved quickly and accurately using readily available open source solvers. Future work will continue to expand these methods by introducing additional, more flexible, shape parameterizations, additional objective functions, and a broader set of geometric constraints.

## References

[1] Hicks, R. M., and Henne, P. A., "Wing Design by Numerical Optimization," *Journal of Aircraft*, Vol. 15, No. 7, 1978, pp. 407–412. https://doi.org/10.2514/3.58379.

[2] Vanderplaats, G., "An efficient algorithm for numerical airfoil optimization," *17th Aerospace Sciences Meeting*, 1979. https://doi.org/10.2514/6.1979-79.

[3] Jameson, A., "Aerodynamic design via control theory," *Journal of Scientific Computing*, Vol. 3, No. 3, 1988, pp. 233–260.

[4] Deng, F., Xue, C., and Qin, N., "Parameterizing Airfoil Shape Using Aerodynamic Performance Parameters," *AIAA Journal*, 2022, pp. 1–14. https://doi.org/10.2514/1.J061464.

[5] Li, J., Bouhlel, M. A., and Martins, J. R. R. A., "Data-Based Approach for Fast Airfoil Analysis and Optimization," *AIAA Journal*, Vol. 57, No. 2, 2019, pp. 581–596. https://doi.org/10.2514/1.J057129.

[6] He, X., Li, J., Mader, C. A., Yildirim, A., and Martins, J. R., "Robust aerodynamic shape optimization—From a circle to an airfoil," *Aerospace Science and Technology*, Vol. 87, 2019, pp. 48–61. https://doi.org/https://doi.org/10.1016/j.ast.2019.01.051.

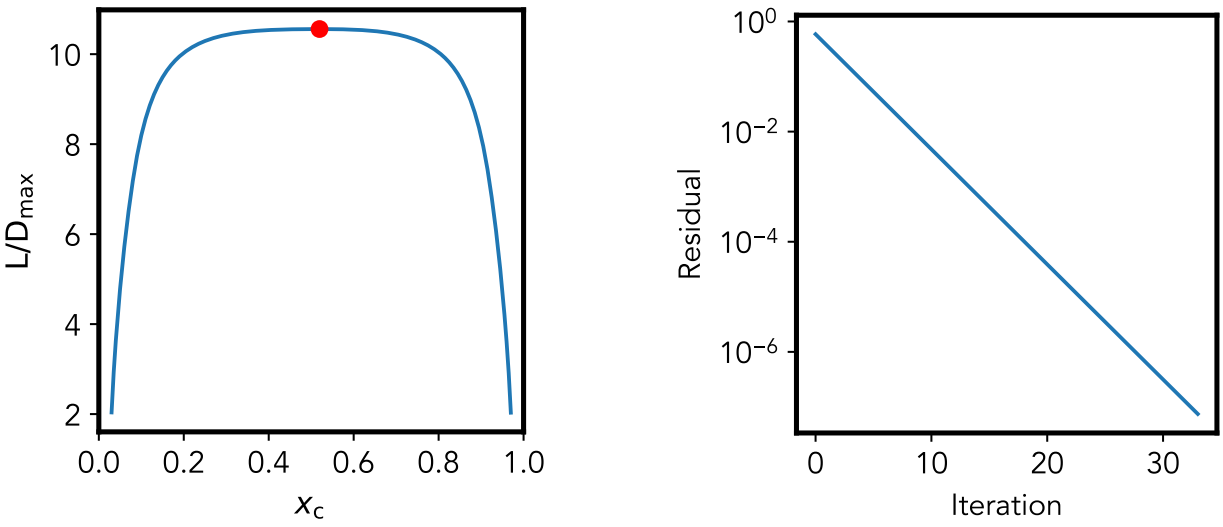


(a) Maximum achievable L/D vs. center of internal payload

(b) Convergence rate of golden search outer optimization loop

**Fig. 7 Optimal airfoil design space and convergence history with variable placement of internal payload**

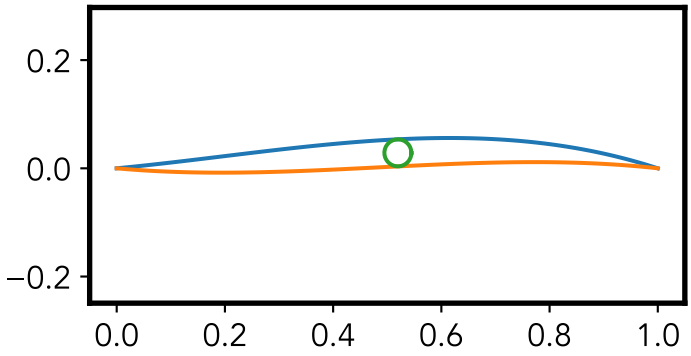


**Fig. 8 Maximum L/D airfoil with optimal internal payload placement**

[7] Meliani, M., Bartoli, N., Lefebvre, T., Bouhlel, M.-A., Martins, J. R. R. A., and Morlier, J., "Multi-fidelity efficient global optimization: Methodology and application to airfoil shape design," *AIAA Aviation 2019 Forum*, 2019. https://doi.org/10.2514/6.2019-3236.

[8] Tyan, M., Park, J.-H., Kim, S., and Lee, J., *Design Optimization of Subsonic Airfoil and Slotted Flap Shape Using Multi-Fidelity Aerodynamic Analysis*, 2013. https://doi.org/10.2514/6.2013-2704.

[9] Sripawadkul, V., Padulo, M., and Guenov, M., "A Comparison of Airfoil Shape Parameterization Techniques for Early Design Optimization," *13th AIAA/ISSMO Multidisciplinary Analysis Optimization Conference*, 2012. https://doi.org/10.2514/6.2010-9050.

[10] Seraj, S., and Martins, J. R., *Aerodynamic Shape Optimization of a Supersonic Transport Considering Low-Speed Stability*, 2021. https://doi.org/10.2514/6.2022-2177.

[11] Wu, N., Mader, C. A., and Martins, J. R. R. A., "A Gradient-based Sequential Multifidelity Approach to Multidisciplinary Design Optimization," *Structural and Multidisciplinary Optimization*, Vol. 65, 2022, pp. 131–151. https://doi.org/10.1007/s00158-022-03204-1.

[12] Liebeck, R. H., *Subsonic Airfoil Design*, 1989, Chap. 5, pp. 133–165. https://doi.org/10.2514/5.9781600865985.0133.0165.

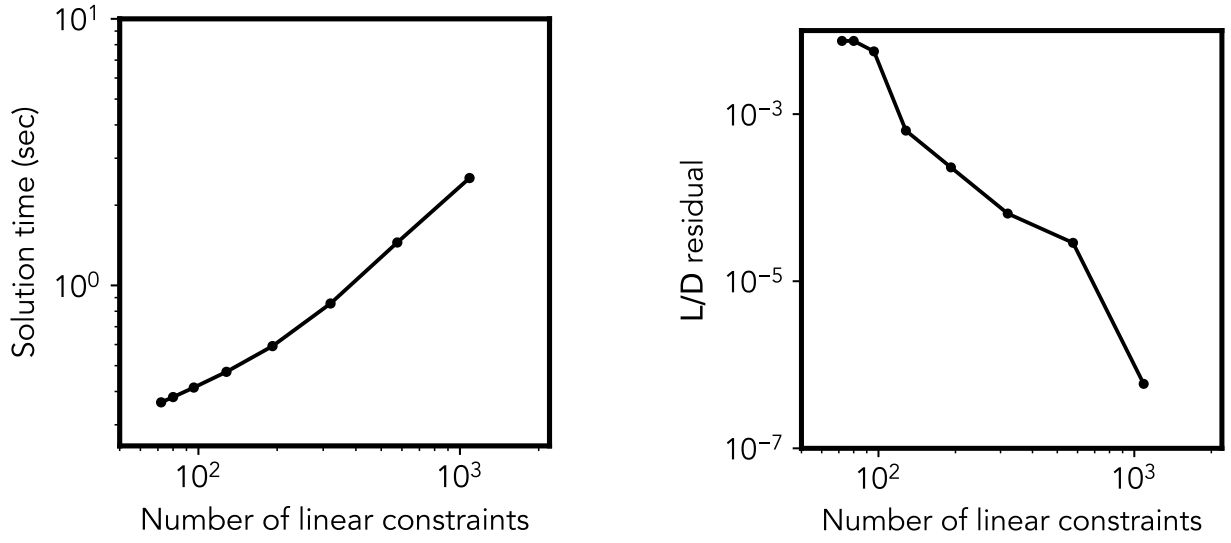


(a) Solution time vs number of linear constraints

(b) Solution residual vs number of constraints

**Fig. 9 Performance history as a function of number of constraints,** 6 **design variables**


[13] Drela, M., *Frontiers of Computational Fluid Dynamics*, 1998, Chap. Pros and Cons of Airfoil Optimization, pp. 363–381. https://doi.org/10.1142/9789812815774_0019.

[14] Drela, M., *Applied Computational Aerodynamics*, 1989, Chap. Elements of Airfoil Design Methodology, pp. 167–189. https://doi.org/10.2514/5.9781600865985.0167.0189.

[15] Martins, J. R. R. A., "Perspectives on aerodynamic design optimization," *AIAA Scitech Forum*, 2020. https://doi.org/10.2514/6.2020-0043.

[16] Boyd, S., and Vandenberghe, L., *Convex Optimization*, Cambridge University Press, 2004.

[17] Angeris, G., Agrawal, A., Evans, A., Chitra, T., and Boyd, S., "Constant Function Market Makers: Multi-Asset Trades via Convex Optimization," , 2021. https://doi.org/10.48550/ARXIV.2107.12484.

[18] Zhu, Z., Schmerling, E., and Pavone, M., "A convex optimization approach to smooth trajectories for motion planning with car-like robots," *IEEE Conference on Decision and Control*, 2015, pp. 835–842. https://doi.org/10.1109/CDC.2015.7402333.

[19] Boyd, S. P., and Kim, S. J., "Geometric Programming for Circuit Optimization," *Proceedings of the 2005 International Symposium on Physical Design*, Association for Computing Machinery, New York, NY, USA, 2005, p. 44–46. https://doi.org/10.1145/1055137.1055148.

[20] Kanno, Y., "Robust truss topology optimization via semidefinite programming with complementarity constraints: a difference-of-convex programming approach," *Computational Optimization and Applications*, Vol. 71, No. 2, 2018, pp. 403–433. https://doi.org/10.1007/s10589-018-0013-3.

[21] Hoburg, W., and Abbeel, P., "Geometric Programming for Aircraft Design Optimization," *AIAA Journal*, Vol. 52, No. 11, 2014, pp. 2414–2426. https://doi.org/10.2514/1.J052732.

[22] Burton, M. J., Drela, M., Courtin, C., Colas, D., Suryakumar, V. S., and Roberts, N. H., *Solar Aircraft Design Trade Studies Using Geometric Programming*, 2018. https://doi.org/10.2514/6.2018-3740.

[23] Zedan, M. F., and Abu-Abdou, K., "Improved thin-airfoil theory," *Journal of Aircraft*, Vol. 25, No. 12, 1988, pp. 1122–1128. https://doi.org/10.2514/3.45711.

[24] Joseph, C., and Mohan, R., "Closed-Form Expressions of Lift and Moment Coefficients for Generalized Camber Using Thin-Airfoil Theory," *AIAA Journal*, Vol. 59, No. 10, 2021, pp. 4264–4270. https://doi.org/10.2514/1.J060859.

[25] Moran, J., *An Introduction to Theoretical and Computational Aerodynamics*, Dover Books on Aeronautical Engineering, Dover Publications, 2013.

[26] Kuethe, A. M., and Chow, C.-y., *Foundations of aerodynamics: Bases of aerodynamic design*, 3rd ed., Wiley New York, 1976.

[27] Diamond, S., and Boyd, S., "CVXPY: A Python-embedded modeling language for convex optimization," *Journal of Machine Learning Research*, Vol. 17, No. 83, 2016, pp. 1–5.

[28] Agrawal, A., Verschueren, R., Diamond, S., and Boyd, S., "A rewriting system for convex optimization problems," *Journal of Control and Decision*, Vol. 5, No. 1, 2018, pp. 42–60.

[29] Löfberg, J., "YALMIP: A toolbox for modeling and optimization in MATLAB," *IEEE International Conference on Robotics and Automation*, 2004, pp. 284–289.